ORIGINAL RESEARCH

# Targeting ATP12A, a Nongastric Proton Pump α Subunit, for Idiopathic Pulmonary Fibrosis Treatment

Mohamed Abdelgied[1], Katie Uhl[1], Oliver G. Chen[1], Chad Schultz[1], Kaylie Tripp[1], Angela M. Peraino[2], Shreya Paithankar[1], Bin Chen[1,3], Maximiliano Tamae Kakazu[2,4], Alicia Castillo Bahena[5], Tara E. Jager[6], Cameron Lawson[6], Dave W. Chesla[5], Nikolay Pestov[7], Nikolai N. Modyanov[7], Jeremy Prokop[1,3], Richard R. Neubig[3], Bruce D. Uhal[8], Reda E. Girgis[2,4,6], and Xiaopeng Li[1]

[1]Department of Pediatrics and Human Development and [4]Department of Medicine, College of Human Medicine, Michigan State University, Grand Rapids, Michigan; [2]Division of Pulmonary and Critical Care Medicine, [5]Research and Development, and [6]Richard Devos Heart and Lung Transplant Program, Spectrum Health, Grand Rapids, Michigan; [3]Department of Pharmacology and Toxicology and [8]Department of Physiology, Michigan State University, East Lansing, Michigan; and [7]Department of Physiology and Pharmacology and Center for Diabetes and Endocrine Research, College of Medicine, University of Toledo, Health Science Campus, Toledo, Ohio

## Abstract

Idiopathic pulmonary fibrosis (IPF) is a pathological condition of unknown etiology that results from injury to the lung and an ensuing fibrotic response that leads to the thickening of the alveolar walls and obliteration of the alveolar space. The pathogenesis is not clear, and there are currently no effective therapies for IPF. Small airway disease and mucus accumulation are prominent features in IPF lungs, similar to cystic fibrosis lung disease. The *ATP12A* gene encodes the α-subunit of the nongastric $H^+$, $K^+$-ATPase, which functions to acidify the airway surface fluid and impairs mucociliary transport function in patients with cystic fibrosis. It is hypothesized that the ATP12A protein may play a role in the pathogenesis of IPF. The authors' studies demonstrate that ATP12A protein is overexpressed in distal small airways from the lungs of patients with IPF compared with normal human lungs. In addition, overexpression of the ATP12A protein in mouse lungs worsened bleomycin induced experimental pulmonary fibrosis. This was prevented by a potassium competitive proton pump blocker, vonoprazan. These data support the concept that the ATP12A protein plays an important role in the pathogenesis of lung fibrosis. Inhibition of the ATP12A protein has potential as a novel therapeutic strategy in IPF treatment.

**Keywords:** pulmonary fibrosis; ATP12A; bleomycin; small airways; proton pump blocker

Approximately 50,000 new patients are diagnosed with idiopathic pulmonary fibrosis (IPF) annually, and ∼40,000 patients die every year from IPF in the United States (1). IPF is a serious health condition that impairs the ability of the lung to exchange oxygen. The exact cause of IPF is unknown, but an injury to the lung can lead to the buildup of fibrotic tissue within the air sacs; as the disease progresses, structures that are crucial to the absorption of oxygen are eventually destroyed (2, 3). The Food and Drug Administration–approved drugs pirfenidone and nintedanib can slow the decline in lung function but cannot reverse the damage that has already been done to the tissue; morbidity and

(Received in original form July 5, 2022; accepted in final form February 13, 2023)

Supported by the National Heart, Lung, and Blood Institute (HL153165-01A1 to X.L.), the Cystic Fibrosis Foundation (LI19XX0), and funds from the Cystic Fibrosis Research Institute and the Spectrum Health-Michigan State University Alliance Corporation.

Author Contributions: M.A., K.U., O.G.C., C.S., K.T., T.E.J., and X.L. participated in the cell culture and biological experiments associated with this study. M.A., K.U., and X.L. were responsible for carrying out all animal protocols and subsequent data analysis. Immunostaining of tissue was performed by M.A. and X.L. RT-PCR was completed by T.E.J. A.M.P., M.T.K., A.C.B., T.E.J., C.L., D.W.C., and R.E.G. obtained informed patient consent and collected human lung tissue samples. K.U., S.P., and B.C. analyzed the RNA-sequencing data and performed differential expression analysis. N.N.M., N.P., J.P., R.R.N., and B.D.U. interpreted the results of the study and contributed to the writing of the manuscript. M.A., K.U., and X.L. wrote the manuscript. All authors read and approved the manuscript before submission.

Correspondence and requests for reprints should be addressed to Xiaopeng Li, Ph.D., Department of Pediatrics and Human Development, College of Human Medicine, Michigan State University, Grand Rapids Research Center, 400 Monroe NW, Office 4008, Grand Rapids, MI 49503. E-mail: lixiao@msu.edu and Reda E. Girgis, M.D., Spectrum Health, Michigan State University College of Human Medicine, 330 Barclay Avenue NW, Suite 200, Grand Rapids, MI 49503. E-mail: reda.girgis@spectrumhealth.org.

This article has a related editorial.

This article has a data supplement, which is accessible from this issue's table of contents online at www.atsjournals.org.

Am J Respir Cell Mol Biol Vol 68, Iss 6, pp 638–650, June 2023

Originally Published in Press as DOI: 10.1165/rcmb.2022-0264OC on February 13, 2023
Internet address: www.atsjournals.org

## Clinical Relevance

This study is conceptually innovative as it provides mechanistic insights into the role of small airways in the pathogenesis of idiopathic pulmonary fibrosis (IPF), which has been rarely investigated and poorly understood despite clinical data suggestive of its importance in IPF pathogenesis. The findings of this study demonstrate the important role of ATP12A in small airways and airway surface liquid pH in the development of IPF and provide a novel therapeutic avenue to target the progressive fibroproliferation of this disease.

mortality remain high (4, 5). Hence, novel therapeutic targets are urgently needed.

The mechanisms underlying the pathogenesis of IPF are unclear (6–8). The main pathologic features include the collapse and obliteration of distal small airways, the proliferation and accumulation of fibroblast and/or myofibroblast cells, and increased collagen deposition in the alveolar spaces (9, 10). Small airways are defined as having a diameter of less than 2 mm in adult human lungs (11). Recent evidence suggests that distal small airways are involved in the early pathogenesis of IPF. Epithelial microfoci of injury and a failure of reepithelization caused by the interplay of genetic predisposition, aging, and environmental factors contribute to fibroblast activation and infiltration of the alveolar spaces (9, 12–14). There is active bronchiolar remodeling, including collagen deposition, found in the small airways of patients with IPF (15–17). Studies on lung explants from patients with IPF compared with controls demonstrate that ~57% of terminal bronchioles are lost in regions of minimal fibrosis, which is associated with the appearance of fibroblastic foci (18, 19). This suggests that the loss of small airways may precede fibrotic changes (18, 19). In addition, Mucin 5B (MUC5B), the gene for major gel-forming mucin, accumulates in distal small airways in patients with IPF. Overexpression of MUC5B leads to mucus accumulation in small airways and enhances bleomycin (BLEO)-induced lung fibrosis (20–22). However, the mechanism behind mucus accumulation in IPF distal lung airways is unclear.

Mucus accumulation is also the main manifestation of cystic fibrosis (CF) lung disease caused by mutations in the CF transmembrane conductance regulator gene. There is a mucociliary transport (MCT) defect in CF airways that is due to lower airway surface liquid (ASL) pH (23). In the present study, we first investigated ATP12A protein expression levels in IPF, chronic obstructive pulmonary disease (COPD), and normal human airways. *ATP12A* genes (previously termed ATP1AL1) encode the catalytic α-subunits of the nongastric $H^+$-$K^+$-ATPases (ngHKAs) (24). ngHKAs represent a third group of potassium-dependent ion-transporting P-type ATPases that are equally distinct from closely related Na, K-ATPases and gastric H, K-ATPases in structure-functional properties (25–27). ATP12A (the catalytic α-subunit) assembles with the β-subunit (ATP1B1), forming an active ion pump (ngHKAs) in the apical membranes of epithelial cells of many different tissues, including colon, kidney, skin, penis, lung, pancreas, and so forth (27–31). The ATP12A protein functions as the α-subunit of a proton pump that acidifies ASL (32). For this study, the use of the term "ATP12A" refers to the α-subunit.

We hypothesize that ATP12A-mediated acid secretion in IPF distal lung small airways may regulate ASL pH, leading to lower ASL pH and impaired MCT and thus contributing to IPF pathophysiology. To test this hypothesis, we evaluated *ATP12A* gene expression in IPF lungs and tested its function in primary cell cultures and animal models. Our findings in this study elucidated a potentially important yet previously underappreciated role of small airway epithelia in the pathogenesis of IPF. Understanding the contribution of small airways and ASL pH to IPF pathogenesis may lead to the discovery of a new therapeutic strategy.

Some of the results of these studies have been previously reported in the form of a preprint (bioRxiv, 8 June 2022; www.biorxiv.org/content/10.1101/2022.06.08.495330v1).

## Methods

### Human Lung Explant Samples

Lung explant samples were obtained from 13 patients with IPF undergoing lung transplantation. Pathologic assessment confirmed findings of advanced usual interstitial pneumonia (UIP) in the subjects with IPF. Control samples ($n = 4$) were obtained from donor lungs that were not suitable for lung transplantation (*see* Table E1 in the data supplement).

### Viral Vectors Mediated ATP12A Expression in Mouse Airways

We promoted ATP12A expression in the airways of male C57BL/6J mice (aged 22 ± 9 wk) through intratracheal instillation of adenovirus subtype 5 encoding mouse ATP12A (ADV-253250; Vector Biolabs) (Ad-ATP12A) with a dose of $10^8$ plaque-forming units per mouse in 50 μl 2% carboxymethylcellulose solution (catalog no. 419273, Sigma-Aldrich). Details for these groups are provided in the data supplement.

### Test Effects of Viral Vector-mediated ATP12A Expression in Mouse Airways with BLEO-induced Pulmonary Fibrosis

Both Ad5 encoding GFP (Ad-GFP) and Ad-ATP12A were administered to mice at a dose of $10^8$ plaque-forming units per mouse in 50 μl 2% carboxymethylcellulose solution by intratracheal instillation. BLEO was administered at a dose of 2 U/kg body weight in 50 μl saline by intratracheal instillation. Details for these groups are provided in the data supplement.

### Test Effects of Inhibition of ATP12A by the Potassium-Competitive Proton Pump Inhibitor (PPI) Vonoprazan (VON) on BLEO-induced Pulmonary Fibrosis in Mice Expressing ATP12A

Because of the sequence similarities, inhibitors for $H^+$, $K^+$-ATPase and $Na^+$, $K^+$-ATPase have some inhibitory effects on ATP12A. PPIs such as SCH-28080 and esomeprazole have been demonstrated to block ATP12A function (33, 34). VON is a $K^+$-competitive PPI that binds to an extracytosolic domain of gastric proton pumps to block their function (35, 36). We tested the effects of VON on BLEO-induced pulmonary fibrosis. VON (100 μM in 50 μl saline) was administered by intratracheal instillation when BLEO or saline was delivered. For the rest of the time course, VON was administered by pharyngeal instillation daily for 13 days. Details for these groups are provided in the data supplement.

### Histochemistry and Immunofluorescence

ATP12A, MUC5B, MUC5AC, and Krt-5 proteins were detected by immunohistochemistry and immunofluorescence.

### *In Situ* Cell Death Detection

The TUNEL kit was used to detect apoptotic cells in mouse lungs. Details are provided in the data supplement.

### *In Situ* Hybridization

RNAScope (Advanced Cell Diagnostics) was used to detect human and mouse ATP12A mRNA, and *in situ* hybridization was performed according to the manufacturer's protocol (Advanced Cell Diagnostics). Details are provided in the data supplement.

### Study Approval

All protocols were performed in compliance with all ethical regulations approved by local institutional review boards; written informed consent was obtained from all patients who participated in the present study (Spectrum Health IRB no.: 2017-198). Studies using animals complied with all relevant ethical regulations. All animal studies were reviewed and approved by the Michigan State University Animal Care and Use Committee (Animal protocol approval no. PROTO201900242).

### Statistical Analysis

Immunofluorescence, *in situ* cell death detection, and Masson trichrome data were analyzed by one-way ANOVA followed by Tukey's multiple comparison *post hoc* test. RT-PCR and the data regarding the number of honeycomb cysts (HCs) were analyzed by paired Student's *t* test using GraphPad Prism, version 9.3.1.

### Data Availability Statement

The data presented in this study are available on request from the corresponding author. Bulk RNA-sequencing (RNA-seq) data are available in the Gene Expression Omnibus database (accession no. GSE205849).

Additional methods can be found in the data supplement.

## Results

### Increased ATP12A Expression in the Small Airways of IPF Lungs

ATP12A is demonstrated to acidify the airway lining fluid and impair MCT function in patients with CF, and it is upregulated in CF large airways (37). We previously reported that ATP12A is not expressed in small airways from normal human distal lungs (38). To test whether ATP12A is expressed in IPF distal lungs, we investigated the expression of ATP12A in lung explant samples collected from patients with advanced IPF ($n = 13$) undergoing lung transplantations. Before enrollment into this study, pathological analysis was performed to confirm a diagnosis of UIP in the IPF samples. Normal lung control samples

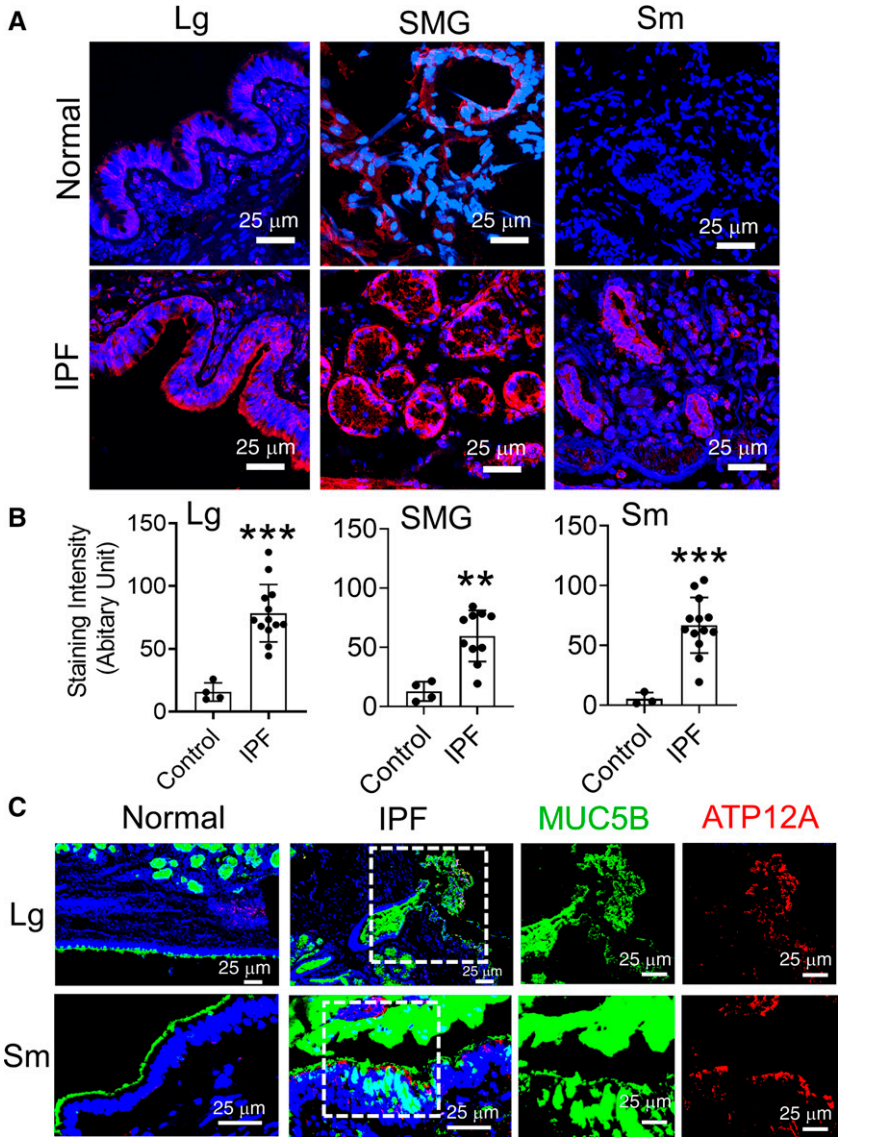


**Figure 1.** ATP12A (adenovirus-expressing mouse ATP12A [Ad-ATP12A]) and MUC5B (Mucin 5B) protein expression in human lung explants. (*A*) Representative confocal microscope images showing immunodetection of ATP12A (red) by immunofluorescence. Nuclei were counterstained by DAPI (blue). Scale bars, 25 μm. Images show the large airways (Lg), SMG, and small airways (Sm) of normal human lungs (upper panel) and human lungs with idiopathic pulmonary fibrosis (IPF) (lower panel). Sm are defined as airways having a diameter that is less than 2 mm. ATP12A overexpression was found in large and Sm as well as in the submucosal glands of IPF. (*B*) ATP12A immunofluorescence staining intensity quantification charts. Data are expressed as mean ± SD of 4 normal and 13 IPF lung samples. At least six lung sections were examined per donor, and ATP12A expression intensity was quantified in more than six Sm per donor. $^{**}P < 0.01$ and $^{***}P < 0.001$, compared with control, respectively. (*C*) Representative confocal microscope images showing immunodetection of ATP12A (red) and MUC5B (green) in Lg and Sm of normal and IPF human lungs. Nuclei were counterstained by DAPI (blue). Scale bars, 25 μm. ATP12A and MUC5B were overexpressed in both Lg and Sm of IPF lungs. The dotted line squares indicate the area in the section that have been magnified to show the co-expression of MUC5B and ATP12A. SMG = submucosal glands.

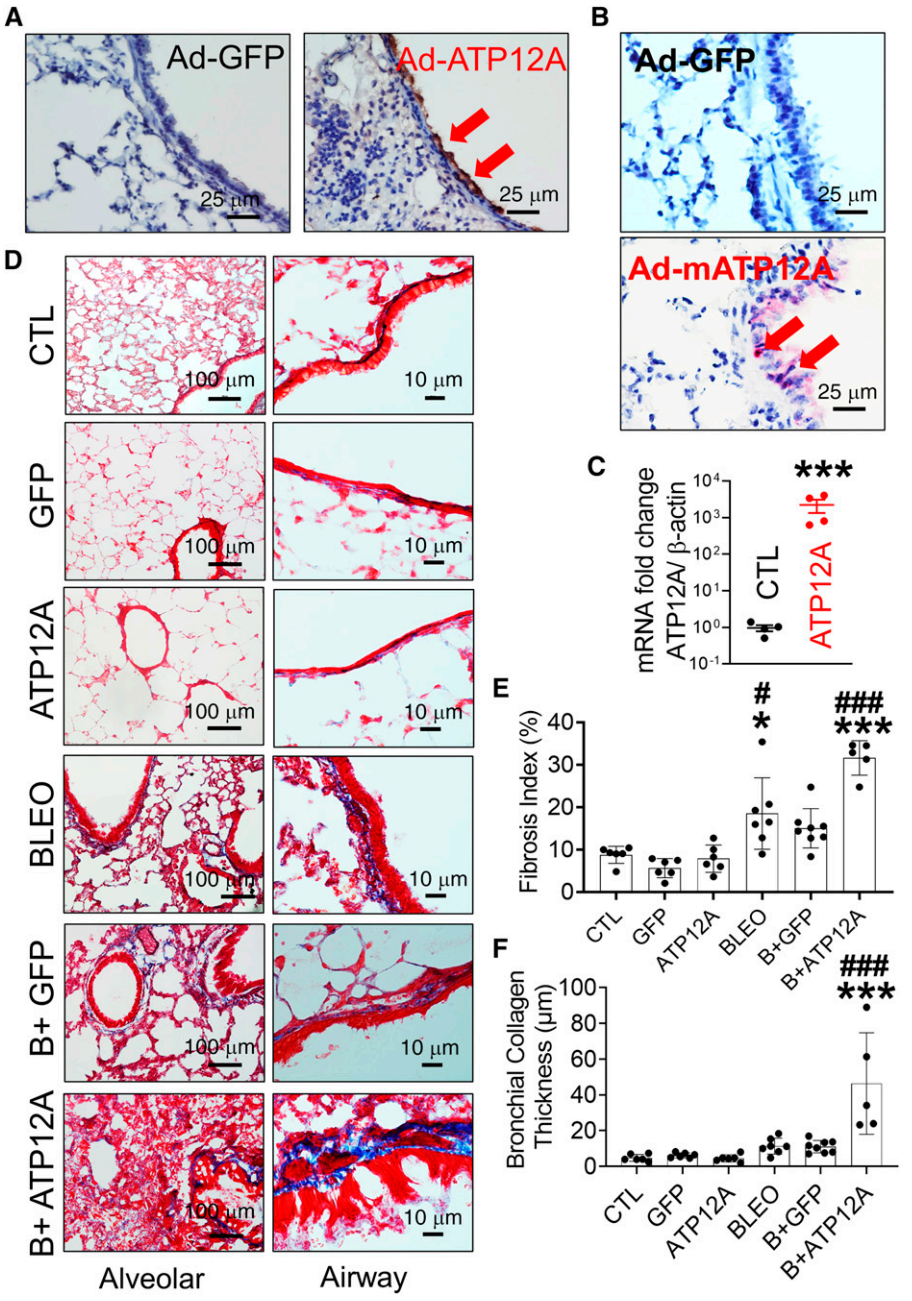


**Figure 2.** Viral vector–mediated ATP12A expression in mouse lungs worsened bleomycin (BLEO)-induced pulmonary fibrosis. (*A*) Brightfield microscope images of Ad-GFP– and Ad-ATP12A–treated mouse lungs show expression of ATP12A in mouse airways (red arrows) (scale bars, 25 μm). (*B*) Brightfield microscope images show ATP12A mRNA detection (red arrows) by *in situ* hybridization. Nuclei were counterstained by hematoxylin (light blue). Scale bars, 25 μm. (*C*) qRT-PCR analysis of *ATP12A* gene expression level in mouse lungs. Data are expressed as mean ± SD. $^{***}P < 0.001$, compared with CTL. (*D*) Bright-field microscope images of mouse lung tissue stained with Masson's trichrome show collagen deposition (blue) in the lung, with the left panel showing collagen deposition throughout the lung (scale bars, 100 μm) and the right panel showing collagen deposition in the peribronchial region (scale bars, 10 μm). (*E*) The chart shows the fibrosis index in the experimental mouse lungs. Data are expressed as mean ± SD. $n \geq 5$ animals per group. (*F*) The chart shows parabronchial collagen thickness (in micrometers) in mouse lungs. Data are expressed as mean ± SD. $n \geq 5$ animals per group. B+ATP12A = BLEO and Ad-ATP12A–treated group; B+GFP = BLEO and Ad-GFP–treated group; CTL = untreated control group; GFP = adenovirus-expressing GFP (Ad-GFP)–treated group. $^{*}P < 0.05$ and $^{***}P < 0.001$, compared with CTL, respectively. $^{\#}P < 0.05$ and $^{\#\#\#}P < 0.001$, compared with BLEO-treated group.

($n = 4$) were collected from donor lungs that did not meet the criteria for transplantation. After dissection of the lungs, samples were fixed and processed for detection of ATP12A, MUC5B, and Mucin 5AC (MUC5AC) by immunofluorescence, immunohistochemistry, and *in situ* hybridization. ATP12A overexpression was detected in both the large airways and submucosal glands (SMGs) and the small airways of IPF lungs. Normal lung large airways, SMGs, and small airways showed a low level of ATP12A expression (Figures 1A and 1B; Figures E1A and E1B). The mean relative staining intensity of ATP12A was 15.6 ± 3.6 in the normal large airway and 78.4 ± 6.4 in IPF large airways. The mean relative staining intensity of ATP12A was 12.9 ± 4.1 in normal lung SMGs and 59.5 ± 6.8 in IPF lung SMGs. The mean relative staining intensity of ATP12A was 5.2 ± 3.0 in the normal small airway and 66.8 ± 6.4 in IPF small airways. Also, IPF large airways, SMGs, and small airways showed an increased expression of MUC5B and MUC5AC compared with those of the normal lungs (Figure 1C; Figure E1C). The surface epithelium of the IPF lungs' small airways showed overexpression of ATP12A associated with MUC5B accumulation (Figure 1C). Those data demonstrated that ATP12A is overexpressed and colocalized with Muc5B accumulation in IPF distal lungs. Those data are consistent with published single-cell RNA-seq data, which demonstrated that ATP12A is mainly upregulated in Muc5B$^{+}$ goblet cells in IPF distal lungs (Figure E2) but not in normal and COPD distal lungs (39).

### Adenovirus-mediated Expression of ATP12A in Mouse Airways Worsened BLEO-induced Pulmonary Fibrosis

Murine airways lack ATP12A expression (32). To mimic the ATP12A expression found in humans, we used intratracheal instillation of adenovirus subtype 5 encoding mouse ATP12A (Ad-ATP12A) to promote the expression of ATP12A in mouse airways. Adenovirus subtype 5 encoding GFP (Ad-GFP) was administered intratracheally in control mice. Fifteen days after instillation, ATP12A expression in mouse airways was confirmed by RT-PCR (Figure 2C) and *in situ* hybridization (Figure 2B). ATP12A protein expression was detected on the apical surface of the mouse airway epithelium as well as in the lung parenchyma (Figure 2A). Additionally, ATP12A mRNA was found in

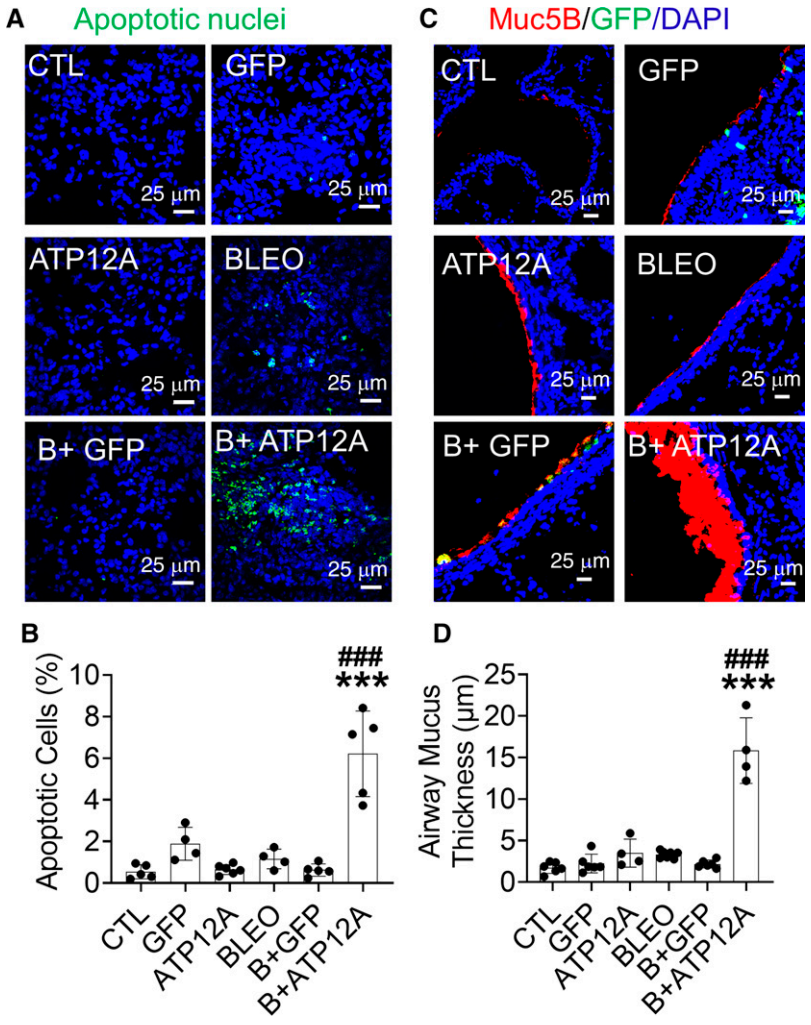


**Figure 3.** Viral vector–mediated ATP12A expression in mouse airways worsens BLEO-induced alveolar epithelium apoptosis and airway mucus accumulation. (*A*) Confocal microscope images show cellular apoptosis of lung epithelial cells by TUNEL staining. Apoptotic cell nuclei are stained green. Scale bars, 25 μm. (*B*) The chart shows the percentage of apoptotic cells in mouse lungs. Data are expressed as mean ± SD, with $n \geq 5$ animals per group. (*C*) Confocal microscope images show immunodetection of MUC5B (red) by immunofluorescence. Nuclei were counterstained by DAPI (blue). Scale bars, 25 μm. (*D*) The chart shows airway mucus thickness in mouse lungs. Data are expressed as mean ± SD. $n \geq 5$ animals per group. $^{***}P < 0.001$, compared with CTL, respectively. $^{###}P < 0.001$, compared with BLEO-treated group.

the airway epithelium (Figure 2B). In contrast, no ATP12A was detected in Ad-GFP–infected mouse lungs, but GFP was expressed in mouse airways (Figure E3).

To determine whether ATP12A plays a role in pulmonary fibrosis, we injured mice with BLEO and assessed the intensity of pulmonary fibrosis indicators. Mice expressing ATP12A showed a significant increase in collagen deposition in the lung (Figures 2D and 2E), apoptosis in the alveolar epithelium (Figures 3A and 3B; Figures E3E and E3F), and accumulation of mucus in airways (Figures 3C and 3D) compared with mice exposed only to BLEO. Mice expressing ATP12A in the lung showed extensive collagen deposition in the lung parenchyma, especially in areas adjacent to the bronchi, with a significant increase in collagen deposition in the peribronchial area (Figures 2D and 2F). Mucus accumulation and airway blockage were also observed in mice expressing ATP12A and challenged with BLEO, which mimicked the mucus accumulation observed in human IPF lung airways (Figures E3G and E3H). ATP12A expression in the apical surface of mouse airway epithelium was associated with airway mucus accumulation (Figure E3G), suggesting that ATP12A has a role in this process.

### Viral Vector-mediated Exogenous ATP12A Expression in Mouse Lungs Enhanced the Fibrotic Pathway and Transforming Growth Factor β1 (TGF-β1) Signaling Pathway in BLEO-induced Pulmonary Fibrosis

To investigate the mechanism of how ATP12A enhances pulmonary fibrosis, bulk RNA-seq was performed to evaluate the mRNA expression in BLEO-induced lung fibrosis in mouse lungs treated with Ad-ATP12A or Ad-GFP (Gene Expression Omnibus accession no. GSE205849). The bulk RNA-seq data for the mouse lung tissue samples were divided into two groups to reduce the batch effect (Figure 4A). Each group consisted of eight mice, with two mice per treatment group. Differential expression analysis of batch 1 revealed 193 differentially expressed genes with a *P* value ⩽0.01; batch 2 had 164 differentially expressed genes with the same *P* value threshold. The gene list for the individual batches was submitted to Ingenuity Pathway Analysis (IPA; QIAGEN) to identify common canonical pathways and common upstream regulators. Batch 1 returned a total of 356 canonical pathways, and the data from batch 2 represented 263 pathways; there were 223 canonical pathways shared between the batches. The same comparison was performed for the upstream regulators, with 294 common regulators identified.

Mouse lungs that had the adenovirus-mediated expression of ATP12A and were challenged with BLEO demonstrated an increase in pathways that are known to play a role in the development of fibrosis. According to the IPA canonical pathway analysis, at least 10 genes are shared between the hepatic fibrosis or hepatic stellate cell activation pathway and the pulmonary fibrosis pathway (Figures 4B and 4E). The shared genes include ACTA2, a key regulator of myofibroblast development; COL1A1; and the transcription factor JUN. These genes are all found to have elevated expression levels in pulmonary fibrosis. Also related to the fibrosis pathway is the actin cytoskeleton signaling pathway, which plays an important role in myofibroblast differentiation.

One of the most noteworthy upstream regulators shared by the two batches of samples is TGF-β1. This protein plays a role in the production of the extracellular matrix,

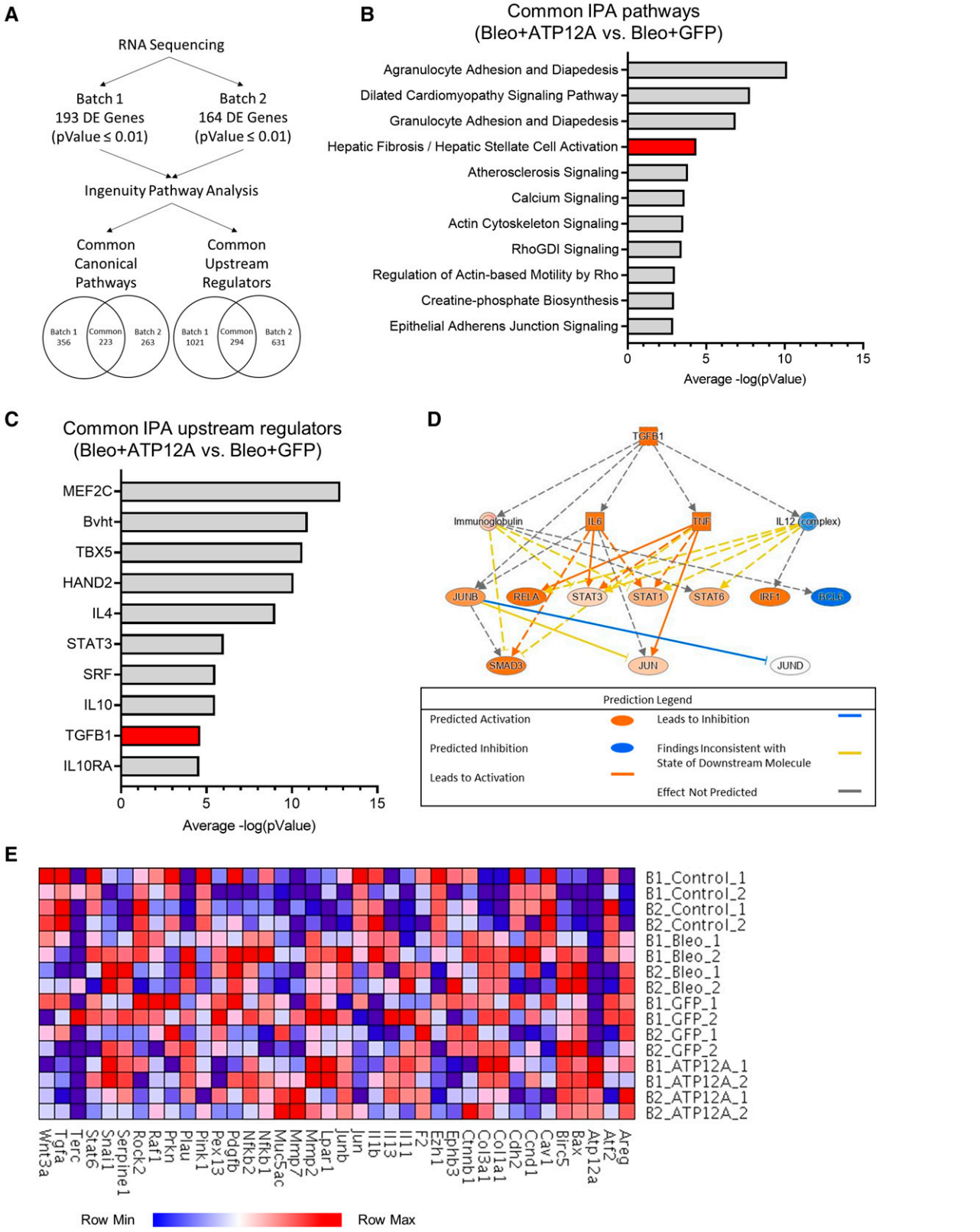


**Figure 4.** Viral vector–mediated ATP12A expression in mouse lungs enhanced fibrotic pathway and transforming growth factor β1 (TGF-β1) signaling pathway in BLEO-induced pulmonary fibrosis. (*A*) Diagram showing the data analysis workflow. Data was collected from the bulk RNA sequencing of mouse lung tissue after treatment with BLEO and the adenovirus-mediated expression of GFP or ATP12A. Sequencing and differential expression analysis were performed on two batches of samples ($P = 0.01$). The lists of differentially expressed genes were submitted to QIAGEN Ingenuity Pathway Analysis (IPA) to identify canonical pathways and upstream regulators. (*B*) The common canonical pathways from

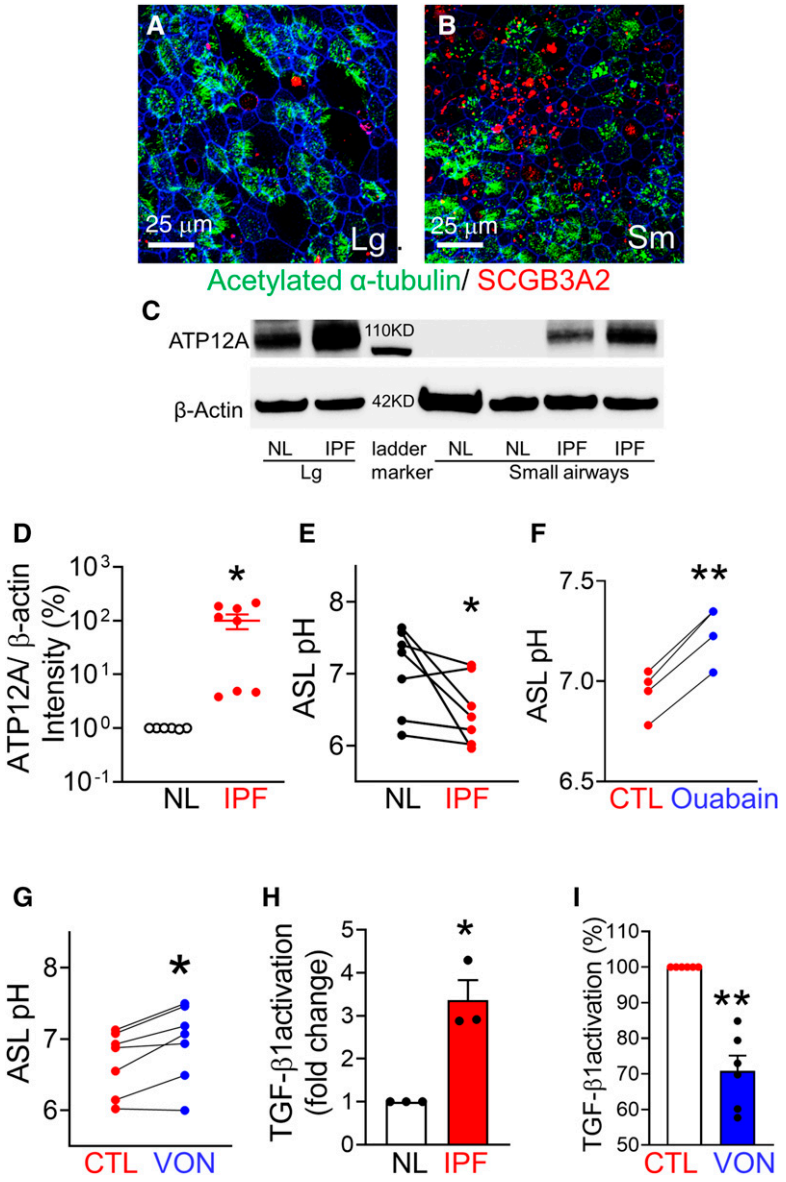


**Figure 5.** ATP12A expression was increased in IPF small airways *in vitro*. (*A* and *B*) Human large (*A*) and small (*B*) airway epithelial cultures. Scale bars, 25 μm. Red indicates small airway epithelial cell marker SCGB3A2, green indicates acetylated α-tubulin, and blue indicates F-actin. (*C*) ATP12 expression was detected by immunoblotting in culture large and small airway cells from normal (NL) and IPF lungs. (*D*) Semiquantification of band intensity showed that ATP12A expression in IPF small airway culture was increased ∼100-fold, compared with NL. $n = 8$. $^{*}P < 0.05$. (*E*) Airway surface liquid (ASL) pH is lower in IPF small airways, compared with normal lung small airways. $n = 9$. $^{*}P < 0.05$. (*F*) Ouabain increased ASL pH in IPF small airways. $n = 4$. $^{**}P < 0.05$ versus CTL. (*G*) Vonoprazan (VON) increased ASL pH in IPF small airways. $n = 7$. $^{*}P < 0.05$ versus CTL. (*H*) IPF small airway apical surface activated more latent TGF-β1. $n = 3$. $^{*}P < 0.05$. (*I*) VON decreased 30% of TGF-β1 activation in IPF small airways. $n = 6$. $^{**}P < 0.01$.

and increased levels of TGF-β1 expression have been reported in pulmonary fibrosis (Figures 4C and 4D). IL-4 was also identified as a common upstream regulator, as well as STAT3. Like TGF-β1, expression levels of IL-4 and STAT3 are increased in patients with pulmonary fibrosis (40, 41). In addition, analysis of the gene expression data for Ad-ATP12A–treated samples revealed the activation of the TGF-β1 signaling pathway. The IPA analysis tool uses its extensive literature-curated database to determine key regulator molecules in a signaling pathway. The TGF-β1 signaling pathway was overlaid with the gene expression data from the two sample batches to predict the activation states of the proteins involved in the pathway (Figure 4D). The IL-12 complex and BCL6 are the only proteins predicted to be inhibited in the BLEO and ATP12A versus BLEO and GFP dataset. TGF-β1, IL-6, TNF, and several members of the STAT family are predicted to be activated. There was not enough power for the analysis tool to predict the state of JUND; however, JUNB, a known inhibitor of JUND, is predicted to be activated. Overall, the treatment of samples with Ad-ATP12A is predicted to activate the TGF-β1 signaling pathway and subsequent downstream molecules.

Moreover, we used the IPA literature database to generate a heatmap of genes associated with the IPF signaling pathway (Figure 4E). A subset of this database was compared with the transcripts per million data from the RNA-seq results for each of the mouse lung samples. We included ATP12A and MUC5AC in the list because of their relevance to this study. ATP12A expression was only present in lung samples of Ad-ATP12A–expressing mice. This is consistent with the literature-supported observation that murine airway cells do not naturally express ATP12A. Lungs treated with BLEO showed increased levels of COL1A1 and COL3A1; a similar trend is observed for the matrix metalloproteins MMP2 and MMP7, with both being more prevalent in samples with viral vector–mediated ATP12A expression (Figure 4E).

**Figure 4.** (*Continued*). the BLEO and ATP12A versus BLEO and GFP comparison in each batch were compiled and arranged according to the average −log(value), as calculated by IPA. The hepatic fibrosis and hepatic stellate cell activation pathway is highlighted in red. (*C*) Common upstream regulators were identified between the BLEO and ATP12A versus BLEO and GFP comparison in the two batches and arranged on the basis of the average −log(pValue) calculated by IPA. The TGF-β1 upstream regulator is highlighted in red. (*D*) Pathway diagram displaying the predicted activation states of molecules in the TGF-β1 signaling pathway based on differential gene expression data submitted to IPA. (*E*) Heatmap displaying the expression levels of selected genes from the IPF pathway, as listed by IPA, as well as genes of interest included by the authors (Atp12A and Muc5ac).

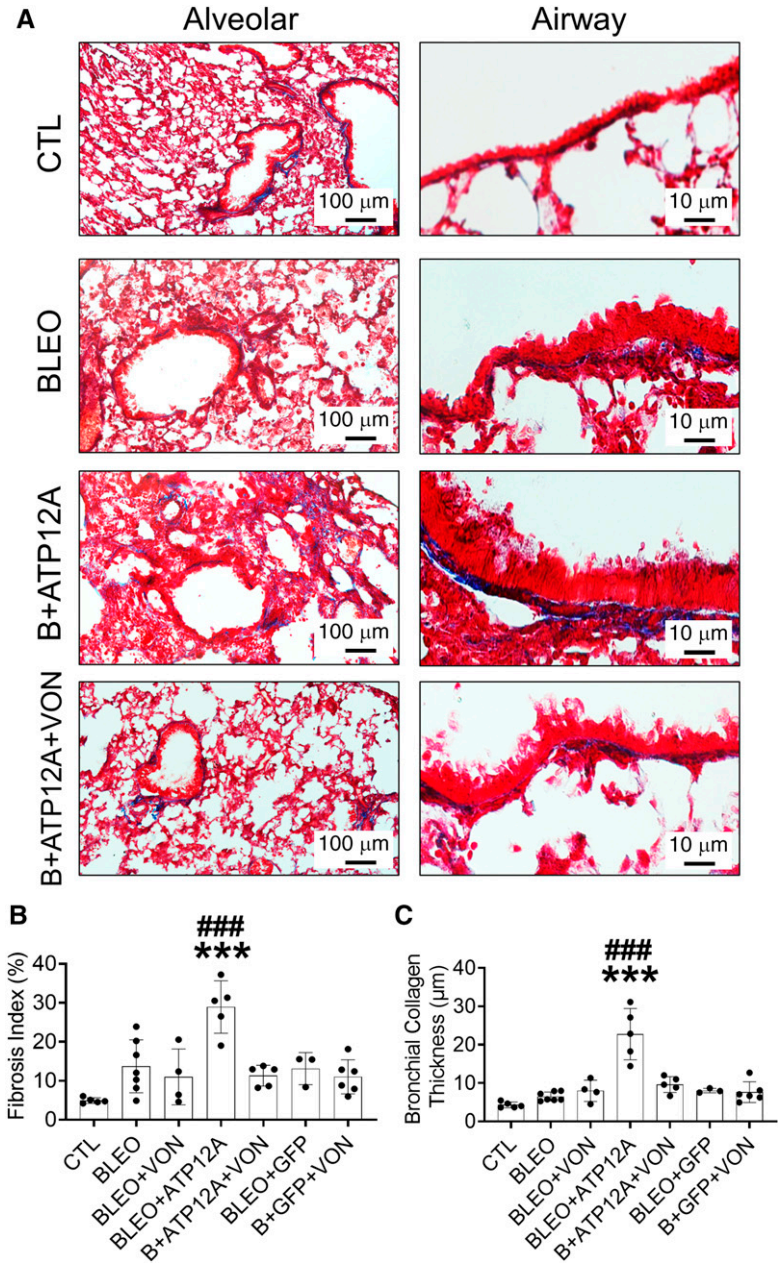


**Figure 6.** Inhibition of ATP12A by potassium-competitive proton pump blocker VON reduced BLEO-induced pulmonary fibrosis in mice expressing ATP12A. (*A*) Bright-field microscope images of mouse lung tissue stained with Masson's trichrome show collagen deposition (blue) in the lung; the left panel shows collagen deposition throughout the lung (scale bars, 100 μm), and the right panel shows collagen deposition in the peribronchial area (scale bars, 10 μm). (*B*) The chart shows the fibrosis index in mouse lungs. Data are expressed as mean ± SD, with $n \geq 5$ animals per group. (*C*) The chart shows parabronchial collagen thickness (in micrometers) in mouse lungs. Data are expressed as mean ± SD. $n \geq 5$ animals per group. $^{***}P < 0.001$ compared to CTL; $^{###}P < 0.001$ compared to B+ATP12A+VON.

### Potassium-Competitive Proton Pump Blocker VON Decreased ASL pH and TGF-β1 Activation in IPF Small Airway Epithelial Cells

To investigate the potential roles of ATP12A in IPF small airways, we developed methods to culture human large and small airway epithelia at the air–liquid interface by adapting a previously published method for culturing pig small airway cells (42). We examined whether human small airway cells can form a well-differentiated epithelium and express small airway–specific genes such as SCGB3A2, a highly expressed secretory protein in human small airways and a marker for small airway epithelial cells (43). In contrast to the minimal expression of SCGB3A2 in the large airway, there is an increased level of SCGB3A2 expression in the human small airway (Figure 5B). Both large and small airway epithelia have abundant acetylated α-tubulin–positive ciliated cells (Figures 5A and 5B), indicating well-differentiated cells. Thus, we validated a human large airway and small airway culture model that preserves the native tissue properties. To test whether small airways from patients with IPF maintain ATP12A expression in primary culture, we examined ATP12A expression by immunoblotting. As expected, robust ATP12A expression was detected in large airway epithelia but was not detected in normal small airway culture. Consistent with immunostaining of ATP12A in IPF lung tissue (Figure 1), there is increased ATP12A expression in IPF small airway culture (Figures 5C and 5D). As ATP12A is upregulated in IPF small airways, we explored the pharmacological methods to inhibit the functions of ATP12A-containing nongastric proton pumps. Because of the sequence similarities, inhibitors for $H^+$, $K^+$-ATPase, and $Na^+$, $K^+$-ATPase have some inhibitory effects on ATP12A with much higher Ki; for example, ouabain is a potent $Na^+$, $K^+$-ATPase inhibitor with Ki (inhibitor constant) of 100 nM but a Ki around 10 μM for ATP12A (44). PPIs of $H^+$, $K^+$-ATPase, such as SCH-28080 and esomeprazole, have been demonstrated to block ATP12 function (33, 34). VON is a $K^+$-competitive PPI that binds to an extracytosolic domain of gastric proton pumps to block their function (35, 36). To test whether ATP12A regulates ASL pH, we tested the effects of both ouabain and VON on ASL pH in IPF small airways. IPF small airways have a lower ASL pH, compared with small airways from normal lungs (Figure 5E). Both ouabain and VON increased ASL pH in IPF small airways (Figures 5F and 4G; Figure E4B). We recently reported that V-type ATPase containing ATP6V0D2 also can contribute to the control of ASL pH in pig small airways (38). However, the V-type ATPase inhibitor bafilomycin does not affect ASL pH in human IPF small airways (Figure E4A). Thus, the data support that ATP12A regulates ASL pH in human small airways from IPF lungs.

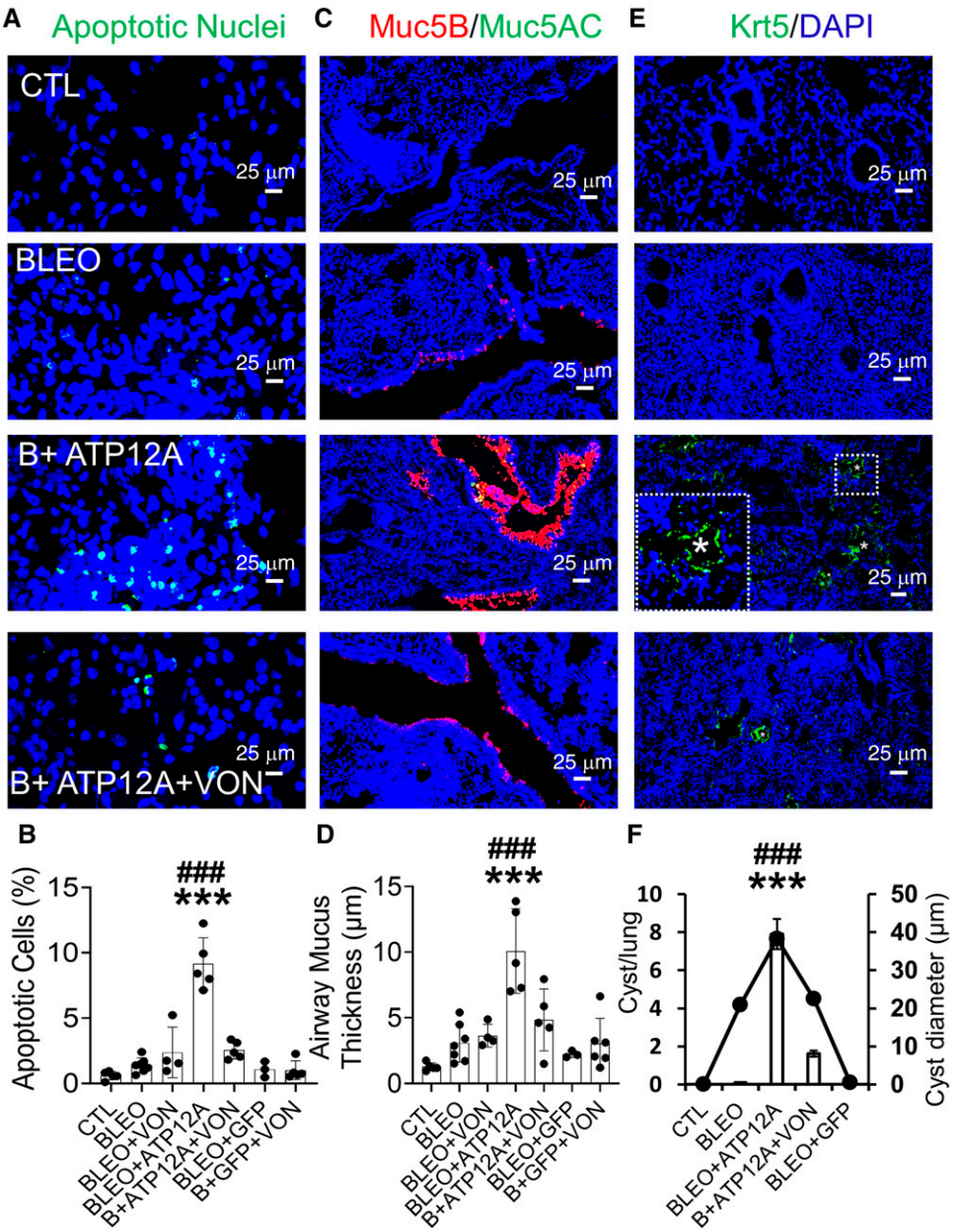


**Figure 7.** Inhibition of ATP12A by potassium-competitive proton pump blocker VON reduced BLEO-induced alveolar epithelium apoptosis, airway mucus accumulation, and honeycomb cyst formation in mice expressing ATP12A. (A) Confocal microscope images show cellular apoptosis of lung epithelial cells by TUNEL staining. Apoptotic cell nuclei are stained green. Scale bars, 25 μm. (*B*) The chart shows the percentage of apoptotic cells in mouse lungs. Data are expressed as mean ± SD. $n \geq 5$ animals per group. (*C*) Confocal microscope images show the immunodetection of MUC5B (red) and MUC5AC (green) by immunofluorescence. Nuclei were counterstained by DAPI (blue). Scale bars, 25 μm. (*D*) The chart shows airway mucus thickness in mouse lungs. Data are expressed as mean ± SD. $n \geq 5$ animals per group. (*E*) Confocal microscope images show immunodetection of keratin 5 (Krt5, basal cell marker in green) by immunofluorescence. The inset shows a honeycomb cyst (white asterisk) with Krt5 + cell lining (green). Nuclei were counterstained by DAPI (blue). Scale bars, 25 μm. (*F*) The chart shows the number of honeycomb cysts per right middle lung lobe (column chart) and the average diameter of honeycomb cysts (linear plot). Data are expressed as mean ± SD. $n \geq 3$ animals per group. $^{***}P < 0.001$ compared to CTL; $^{\#\#\#}P < 0.001$ compared to B+ATP12A+VON.

Because data in Figure 4 demonstrated that viral-mediated expression of ATP12A enhanced BLEO-induced lung fibrosis and activation of the TGF-β1 signaling pathway (Figure 4), we hypothesized that ATP12A may play a role in latent TGF-β1 activation. To investigate the potential role of ATP12A in IPF small airways, we developed an assay to compare the activation of latent TGF-β1 in small airway epithelia from IPF and normal lungs. Latent TGF-β1 (catalog no. 299-LT-005/CF; R&D Systems) was applied to the apical surface for 24 hours; the activated TGF-β1 was quantified by a TGF-β1 ELISA kit. Small airway epithelial cells

from IPF lungs activated almost threefold more latent TGF-β1 compared with small airways from normal lungs (Figure 5H). In addition, the pharmacological inhibitor VON reduced the rate of TGF-β1 activation by 25% in IPF small airways (Figure 5I). However, VON does not affect TGF-β1 activation in small airways from normal lungs (Figure E4C). Together, these data suggest that VON may have antifibrotic roles *in vivo*.

### Inhibition of ATP12A by Potassium-Competitive Proton Pump Blocker Vonoprazan Reduced BLEO-induced Pulmonary Fibrosis in Mice Expressing ATP12A

To confirm whether ATP12A expression has a role in the enhancement of BLEO-induced pulmonary fibrosis in mice, we inhibited the function of ATP12A by using VON as a nongastric proton pump inhibitor. It has been reported that VON has a more potent and longer lasting inhibitory effect on gastric acid secretion in animal models (45), compared with other traditional PPIs, such as esomeprazole. The efficacy of VON is not dependent on low pH in the stomach, so it would be advantageous to test intratracheal administration to avoid systemic side effects. Mice were administered VON daily by means of the oropharyngeal aspiration route for the duration of the experiment. In oropharyngeal aspiration, the drug is put into a suspension, and the treatment is administered to mice through reflexive aspiration. Our data shows that VON significantly inhibited the effects of ATP12A expression on BLEO-induced pulmonary fibrosis. The lungs of these VON-treated mice showed significant reductions in pulmonary collagen deposition (Figures 6A–6C; Figures E5A and E5B), apoptosis in the alveolar epithelium (Figures 7A and 7B; Figure E5C), airway mucous thickness (Figures 7C and 7D; Figure E5D), and HC formation (Figures 7E and 7F; Figure E5E) compared with the saline-treated group.

## Discussion

In the present study, we first investigated ATP12A expression levels in IPF and normal human airways. It is interesting that we found clear evidence of ATP12A overexpression in IPF small airway surface epithelium and HCs lining the epithelium. Moreover, MUC5B overexpression was observed in IPF small airways in association with ATP12A upregulation. Overexpression of ATP12A in mouse lungs aggravated pulmonary fibrosis (PF) in a BLEO-induced experimental model of PF, which was blocked by the potassium-competitive PPI VON. These data support the hypothesis that ATP12A plays an important role in the pathogenesis of lung fibrosis. Our overall conclusion is that ATP12A-mediated acid secretion in IPF small airways and distal lungs decreases ASL pH, impairs MCT, increases pH-dependent TGF-β1 activation, and enhances mucus accumulation and lung fibrosis; these effects can be blocked by the potassium-competitive proton pump blocker VON.

### Role of ATP12A in Lung Diseases

ATP12A serves as the main proton pump by moving protons out of epithelial cells in exchange for $K^+$ to acidify ASL in large airway epithelia (23, 32, 46–48). ATP12A is required for CF lung disease development, as it is responsible for proton secretions and the subsequent ASL acidification in the airways of patients with CF (32, 49). Mouse lungs lack ATP12A expression; therefore, CF mice do not demonstrate all the characteristics of CF lung disease. The expression of ATP12A is upregulated in large airways of patients with CF (37). Overexpression of ATP12A in CF mouse lungs decreases ASL pH and impairs bacterial eradication abilities (32). Additionally, ATP12A was shown to be a regulator of ASL viscosity, and ATP12A upregulation was associated with an increased ASL viscosity in CF large airways which was restored through the inhibition of ATP12A by ouabain (50). Similarly, upregulation of ATP12A expression in IPF small airways may increase mucus viscosity by impacting mucin biochemistry and structure through alterations in the luminal composition or the pH of secretory vesicles (51, 52). Airway epithelial secretions, including airway mucus, are prominent $H^+/HCO_3^-$ buffers; therefore, ATP12A overexpression-driven proton secretion into the airways may increase airway mucus oxidation (53). This, in turn, increases mucin polymer disulfide cross-links that increase the viscosity and stiffen airway mucus (32, 49, 50, 54). It is reported that ASL pH is decreased in CF small airways (38), and we demonstrated that ATP12A is upregulated and that ASL pH is lower in IPF small airways in this study. Muc5B overexpression is the most relevant feature shared between CF and IPF (55), thus lower ASL pH might be one of the shared underlying mechanisms. It is known that distal small airway epithelial cells in both IPF and COPD lungs lose normal proximal to distal differentiation patterns (56, 57), but ATP12A is not upregulated in COPD distal lungs (Figure E2). This suggests that upregulation of ATP12A in IPF small airways is not a "bystander" effect of the bronchiolization that occurs in IPF; otherwise, ATP12A would be upregulated in COPD distal lungs. The detailed mechanism of upregulation of ATP12A in IPF distal small airways will need further studies.

Similar to CF lung disease, the hypersecretion and accumulation of mucus and mucociliary clearance impairment are common characteristics found in human patients with IPF (21, 58). The major potential consequence of mucus accumulation and ciliary impairment, (resulting from the increased mucus viscosity) is the retention of inhaled foreign substances (air pollutants, microorganisms, etc.), which initiates chronic inflammation in alveolar regions and reduces lung functions (59). Also, mucus accumulation may promote mucus aspiration into distal airways, impairing the gas exchange process (60). Aspirated mucus may cause alveolar injury either by disrupting the surfactant surface tension properties or through interference with the interaction between alveolar type II cells and the underlying matrix (61). These alveolar injuries, over time, could lead to progressive fibroproliferation; microscopic scarring; and, eventually, IPF development (62, 63). Our findings demonstrate that ATP12A-expressing mice showed significant accumulation of mucin and airway mucus plugging after BLEO exposure, which was prevented by inhibition of ATP12A activity by VON. Additionally, the coexpression of both ATP12A and MUC5B in the distal airways and the observed airway mucus buildup and plugging in mice expressing ATP12A after being injured with BLEO support the critical role of ATP12A in the pathogenesis of pulmonary fibrosis.

HCs are clusters of fibrotic airspaces characteristic of the UIP observed in IPF. They are lined with pseudostratified columnar ciliated epithelium over cytokeratin 5–expressing basal cells and filled with mucus. It is interesting that we observed a significant number of HCs in mice expressing ATP12A 14 days after exposure to a single dose of BLEO by intratracheal

instillation, which is not observed in the conventional BLEO model. HCs were induced in the chronic phase after a single dose of BLEO exposure (58, 64). Further, it has been reported that MUC5B overexpression can elicit HC formation in the BLEO model and that the severity of pulmonary fibrosis and HC formation was correlated with the degree of MUC5B expression (58). In the present study, when ATP12A-overexpressing mouse lungs were challenged with BLEO, it resulted in MUC5B overexpression in airways, which induced early HC development.

To further confirm whether the enhancement of pulmonary fibrosis observed in mice expressing ATP12A after BLEO exposure was ATP12A related, we inhibited the action of ATP12A through oropharyngeal administration of VON. VON is a novel oral potassium-competitive acid blocker that competitively blocks the potassium binding site of $H^+$-$K^+$ ATPases (65, 66). Because of its higher pKa (acid-base dissociation constant) value, VON has a more stable inhibitory effect on gastric acid secretions than conventional PPIs and is commonly used in the treatment of peptic ulcers, gastroesophageal reflux, and *Helicobacter pylori* eradication (65, 67–71). PPIs have been commonly used in IPF clinical treatment guidelines in many countries (72). In this study, VON administration significantly inhibited the synergistic effect of ATP12A expression on BLEO-induced pulmonary fibrosis in mice. Although other traditional PPIs such as esomeprazole have been used to attenuate BLEO-induced PF through other mechanisms (73), systemic delivery by oral administration may have some side effects, as PPIs will inhibit gastric acid secretion. The efficacy of VON is not dependent on low pH in the stomach, so it will be advantageous to test intratracheal administration. As shown in Figure 5, VON only had an antifibrotic effect in the group of BLEO+Ad-ATP12A. This suggests that VON, when administered intratracheally, has different mechanisms than systemically orally administered esomeprazole. VON was recently approved by the Food and Drug Administration under the brand name VOQUEZNA, with one or two antibiotic combinations for the treatment of *H. pylori* infection in adults (74). Our findings support the important role of ATP12A in the development of pulmonary fibrosis, and VON could be repurposed or reformulated for IPF clinical trials.

### TGF-β1 Activation and Its Role in Lung Fibrosis

TGF-β1 is the essential profibrotic cytokine, and its overactivation mediates the development of PF (75–77). Latent TGF-β1 is synthesized by various cell types in fibrotic lungs, including epithelial cells and myofibroblasts. The latent precursor form can be activated by various mechanisms: integrins, proteases, reactive oxygen species, mechanical stress, and low pH (78). Activation of latent TGF-β1 is critical for all downstream profibrotic effects. Notably, it has been reported that low pH can increase activation of latent TGF-β1 (79–82). We demonstrated that small airways from IPF lungs express upregulated ATP12A with lower ASL pH, and there is more latent TGF-β1 activation that can be partially blocked by VON. This evidence supports the hypothesis that a lower pH microenvironment in distal lungs contributes to lung fibrosis pathogenesis. We did not explore the mechanism of pH-dependent change in the affinity to the TGF receptors in the apical membrane (83), but it should prove to be a promising direction for future study.

### Apoptosis of Distal Airway and Alveolar Epithelial Cells Is Involved in Pulmonary Fibrogenesis

As apoptosis is a highly regulated physiological process of cell removal, it plays a fundamental role in the homeostatic control of the cell population (84). An increase in the incidence of apoptosis within a given cell population can result in considerable cell loss over time. Therefore, upregulated apoptosis is likely to account for the excessive loss of alveolar epithelial cells or the failure to re-epithelize, which is characteristic of pulmonary fibrosis. Studies in our labs and others using BLEO-treated rat and mouse models strongly support the role of epithelial apoptosis as a profibrotic event in fibrogenesis (85). Collagen deposition and epithelial apoptosis induced by BLEO in rats and mice were blocked by ZVADfmk, a broad-spectrum inhibitor of caspase, one of the key enzymes mediating apoptosis (86, 87). In the present study, we detected increased apoptosis in ATP12A-overexpressing mice treated with BLEO, which can be prevented by VON. We speculate that lower pH in distal lungs enhances apoptosis, which is also a contributor to the fibrogenic process in both human lungs and animal models (88–90).

In summary, this study is conceptually innovative, as it provides mechanistic insights into the role of small airways in the pathogenesis of IPF, which has been rarely investigated and poorly understood, despite clinical data suggestive of its importance in IPF pathogenesis. The potential roles of ATP12A in the pathogenesis of IPF are summarized in Figure E6. The findings of this study demonstrate the important role of small airways and ASL pH in the development of IPF and provide support for a novel therapeutic avenue to target the progressive fibroproliferation of this disease. ■

**Author disclosures** are available with the text of this article at www.atsjournals.org.

**Acknowledgment:** The authors appreciate the help and assistance of Lung Bioengineering, Inc., and are deeply grateful to the persons who donated their lungs for these studies.

## References

1. Blackwell TS, Tager AM, Borok Z, Moore BB, Schwartz DA, Anstrom KJ, *et al.* Future directions in idiopathic pulmonary fibrosis research. An NHLBI workshop report. *Am J Respir Crit Care Med* 2014;189: 214–222.
2. Pardo A, Selman M. The interplay of the genetic architecture, aging, and environmental factors in the pathogenesis of idiopathic pulmonary fibrosis. *Am J Respir Cell Mol Biol* 2021;64:163–172.
3. Fonseca C, Abraham D, Black CM. Lung fibrosis. *Springer Semin Immunopathol* 1999;21:453–474.
4. King TE Jr, Albera C, Bradford WZ, Costabel U, du Bois RM, Leff JA, *et al.* All-cause mortality rate in patients with idiopathic pulmonary fibrosis. Implications for the design and execution of clinical trials. *Am J Respir Crit Care Med* 2014;189:825–831.
5. Richeldi L, du Bois RM, Raghu G, Azuma A, Brown KK, Costabel U, *et al.*; INPULSIS Trial Investigators. Efficacy and safety of nintedanib in idiopathic pulmonary fibrosis. *N Engl J Med* 2014;370:2071–2082.
6. Mason RJ, Schwarz MI, Hunninghake GW, Musson RA. NHLBI Workshop Summary. Pharmacological therapy for idiopathic pulmonary fibrosis. Past, present, and future. *Am J Respir Crit Care Med* 1999;160: 1771–1777.

7. Crystal RG, Bitterman PB, Mossman B, Schwarz MI, Sheppard D, Almasy L, *et al.* Future research directions in idiopathic pulmonary fibrosis: summary of a National Heart, Lung, and Blood Institute working group. *Am J Respir Crit Care Med* 2002;166:236–246.
8. Feghali-Bostwick C. Pulmonary fibrosis: something old, something new… still waiting for a breakthrough. *Am J Physiol Lung Cell Mol Physiol* 2020;319:L560–L561.
9. Selman M, Pardo A. Idiopathic pulmonary fibrosis: an epithelial/fibroblastic cross-talk disorder. *Respir Res* 2002;3:3.
10. Lipinski JH, Moore BB, O'Dwyer DN. The evolving role of the lung microbiome in pulmonary fibrosis. *Am J Physiol Lung Cell Mol Physiol* 2020;319:L675–L682.
11. Hogg JC, Macklem PT, Thurlbeck WM. Site and nature of airway obstruction in chronic obstructive lung disease. *N Engl J Med* 1968; 278:1355–1360.
12. Haschek WM, Witschi H. Pulmonary fibrosis—a possible mechanism. *Toxicol Appl Pharmacol* 1979;51:475–487.
13. Witschi H. Responses of the lung to toxic injury. *Environ Health Perspect* 1990;85:5–13.
14. Le Saux CJ, Chapman HA. Idiopathic pulmonary fibrosis: cell death and inflammation revisited. *Am J Respir Cell Mol Biol* 2018;59:137–138.
15. Parra ER, Noleto GS, Tinoco LJ, Capelozzi VL. Immunophenotyping and remodeling process in small airways of idiopathic interstitial pneumonias: functional and prognostic significance. *Clin Respir J* 2008; 2:227–238.
16. Figueira de Mello GC, Ribeiro Carvalho CR, Adib Kairalla R, Nascimento Saldiva PH, Fernezlian S, Ferraz Silva LF, *et al.* Small airway remodeling in idiopathic interstitial pneumonias: a pathological study. *Respiration* 2010;79:322–332.
17. Pappas K. Bronchiolitis and bronchial disorders in interstitial lung disease. *Curr Opin Pulm Med* 2011;17:316–324.
18. Verleden SE, Tanabe N, McDonough JE, Vasilescu DM, Xu F, Wuyts WA, *et al.* Small airways pathology in idiopathic pulmonary fibrosis: a retrospective cohort study. *Lancet Respir Med* 2020;8: 573–584.
19. Tanabe N, McDonough JE, Vasilescu DM, Ikezoe K, Verleden SE, Xu F, *et al.* Pathology of idiopathic pulmonary fibrosis assessed by a combination of microcomputed tomography, histology, and immunohistochemistry. *Am J Pathol* 2020;190:2427–2435.
20. Seibold MA, Wise AL, Speer MC, Steele MP, Brown KK, Loyd JE, *et al.* A common MUC5B promoter polymorphism and pulmonary fibrosis. *N Engl J Med* 2011;364:1503–1512.
21. Hancock LA, Hennessy CE, Solomon GM, Dobrinskikh E, Estrella A, Hara N, *et al.* Muc5b overexpression causes mucociliary dysfunction and enhances lung fibrosis in mice. *Nat Commun* 2018;9:5363.
22. Schwartz DA. Idiopathic pulmonary fibrosis is a genetic disease involving mucus and the peripheral airways. *Ann Am Thorac Soc* 2018;15: S192–S197.
23. Stoltz DA, Meyerholz DK, Welsh MJ. Origins of cystic fibrosis lung disease. *N Engl J Med* 2015;372:351–362.
24. Crambert G. H,K-ATPases in epithelia. In: Hamilton KL, Devor DC, editors. Studies of epithelial transporters and ion channels. Ion channels and transporters of epithelia in health and disease, 2nd ed. Vol. 3. Cham: Springer; 2020. pp. 425–445.
25. Modyanov NN, Petrukhin KE, Sverdlov VE, Grishin AV, Orlova MY, Kostina MB, *et al.* The family of human Na,K-ATPase genes. ATP1AL1 gene is transcriptionally competent and probably encodes the related ion transport ATPase. *FEBS Lett* 1991;278:91–94.
26. Modyanov NN, Mathews PM, Grishin AV, Beguin P, Beggah AT, Rossier BC, *et al.* Human ATP1AL1 gene encodes a ouabain-sensitive H-K-ATPase. *Am J Physiol* 1995;269:C992–C997.
27. Crowson MS, Shull GE. Isolation and characterization of a cDNA encoding the putative distal colon H+,K(+)-ATPase. Similarity of deduced amino acid sequence to gastric H+,K(+)-ATPase and Na+,K(+)-ATPase and mRNA expression in distal colon, kidney, and uterus. *J Biol Chem* 1992;267:13740–13748.
28. Pestov NB, Korneenko TV, Radkov R, Zhao H, Shakhparonov MI, Modyanov NN. Identification of the β-subunit for nongastric H-K-ATPase in rat anterior prostate. *Am J Physiol Cell Physiol* 2004;286: C1229–C1237.
29. Pestov NB, Korneenko TV, Adams G, Tillekeratne M, Shakhparonov MI, Modyanov NN. Nongastric H-K-ATPase in rodent prostate: lobe-specific expression and apical localization. *Am J Physiol Cell Physiol* 2002;282:C907–C916.
30. Pestov NB, Korneenko TV, Shakhparonov MI, Shull GE, Modyanov NN. Loss of acidification of anterior prostate fluids in Atp12a-null mutant mice indicates that nongastric H-K-ATPase functions as proton pump in vivo. *Am J Physiol Cell Physiol* 2006;291:C366–C374.
31. Pestov NB, Romanova LG, Korneenko TV, Egorov MV, Kostina MB, Sverdlov VE, *et al.* Ouabain-sensitive H,K-ATPase: tissue-specific expression of the mammalian genes encoding the catalytic alpha subunit. *FEBS Lett* 1998;440:320–324.
32. Shah VS, Meyerholz DK, Tang XX, Reznikov L, Abou Alaiwa M, Ernst SE, *et al.* Airway acidification initiates host defense abnormalities in cystic fibrosis mice. *Science* 2016;351:503–507.
33. Modyanov NN, Mathews PM, Grishin AV, Beguin P, Beggah AT, Rossier BC, *et al.* Human ATP1AL1 gene encodes a ouabain-sensitive H-K-ATPase. *Am J Physiol* 1995;269:C992–C997.
34. Delpiano L, Thomas JJ, Yates AR, Rice SJ, Gray MA, Saint-Criq V. Esomeprazole increases airway surface liquid ph in primary cystic fibrosis epithelial cells. *Front Pharmacol* 2018;9:1462.
35. Scott DR, Munson KB, Marcus EA, Lambrecht NWG, Sachs G. The binding selectivity of vonoprazan (TAK-438) to the gastric $H^+$, $K^+$-ATPase. *Aliment Pharmacol Ther* 2015;42:1315–1326.
36. Abe K, Irie K, Nakanishi H, Suzuki H, Fujiyoshi Y. Crystal structures of the gastric proton pump. *Nature* 2018;556:214–218.
37. Scudieri P, Musante I, Caci E, Venturini A, Morelli P, Walter C, *et al.* Increased expression of ATP12A proton pump in cystic fibrosis airways. *JCI Insight* 2018;3:e123616.
38. Li X, Villacreses R, Thornell IM, Noriega J, Mather S, Brommel CM, *et al.* V-type ATPase mediates airway surface liquid acidification in pig small airway epithelial cells. *Am J Respir Cell Mol Biol* 2021;65:146–156.
39. Neumark N, Cosme C Jr, Rose KA, Kaminski N. The idiopathic pulmonary fibrosis cell atlas. *Am J Physiol Lung Cell Mol Physiol* 2020; 319:L887–L893.
40. Huaux F, Liu T, McGarry B, Ullenbruch M, Phan SH. Dual roles of IL-4 in lung injury and fibrosis. *J Immunol* 2003;170:2083–2092.
41. Pedroza M, Le TT, Lewis K, Karmouty-Quintana H, To S, George AT, *et al.* STAT-3 contributes to pulmonary fibrosis through epithelial injury and fibroblast-myofibroblast differentiation. *FASEB J* 2016;30:129–140.
42. Li X, Tang XX, Vargas Buonfiglio LG, Comellas AP, Thornell IM, Ramachandran S, *et al.* Electrolyte transport properties in distal small airways from cystic fibrosis pigs with implications for host defense. *Am J Physiol Lung Cell Mol Physiol* 2016;310:L670–L679.
43. Reynolds SD, Reynolds PR, Pryhuber GS, Finder JD, Stripp BR. Secretoglobins SCGB3A1 and SCGB3A2 define secretory cell subsets in mouse and human airways. *Am J Respir Crit Care Med* 2002;166: 1498–1509.
44. Adams G, Tillekeratne M, Yu C, Pestov NB, Modyanov NN. Catalytic function of nongastric H,K-ATPase expressed in Sf-21 insect cells. *Biochemistry* 2001;40:5765–5776.
45. Hori Y, Matsukawa J, Takeuchi T, Nishida H, Kajino M, Inatomi N. A study comparing the antisecretory effect of TAK-438, a novel potassium-competitive acid blocker, with lansoprazole in animals. *J Pharmacol Exp Ther* 2011;337:797–804.
46. Simonin J, Bille E, Crambert G, Noel S, Dreano E, Edwards A, *et al.* Airway surface liquid acidification initiates host defense abnormalities in cystic fibrosis. *Sci Rep* 2019;9:6516.
47. Burnay M, Crambert G, Kharoubi-Hess S, Geering K, Horisberger J-D. *Bufo marinus* bladder H-K-ATPase carries out electroneutral ion transport. *Am J Physiol Renal Physiol* 2001;281:F869–F874.
48. Coakley RD, Grubb BR, Paradiso AM, Gatzy JT, Johnson LG, Kreda SM, *et al.* Abnormal surface liquid pH regulation by cultured cystic fibrosis bronchial epithelium. *Proc Natl Acad Sci USA* 2003;100:16083–16088.
49. Shah VS, Ernst S, Tang XX, Karp PH, Parker CP, Ostedgaard LS, *et al.* Relationships among CFTR expression, $HCO_3^-$ secretion, and host defense may inform gene- and cell-based cystic fibrosis therapies. *Proc Natl Acad Sci USA* 2016;113:5382–5387.
50. Lennox AT, Coburn SL, Leech JA, Heidrich EM, Kleyman TR, Wenzel SE, *et al.* ATP12A promotes mucus dysfunction during type 2 airway inflammation. *Sci Rep* 2018;8:2109.
51. Chen EY, Yang N, Quinton PM, Chin WC. A new role for bicarbonate in mucus formation. *Am J Physiol Lung Cell Mol Physiol* 2010;299: L542–L549.

52. Verdugo P, Aitken M, Langley L, Villalon MJ. Molecular mechanism of product storage and release in mucin secretion. II. The role of extracellular Ca++. *Biorheology* 1987;24:625–633.
53. Kim D, Liao J, Hanrahan JW. The buffer capacity of airway epithelial secretions. *Front Physiol* 2014;5:188.
54. Yuan S, Hollinger M, Lachowicz-Scroggins ME, Kerr SC, Dunican EM, Daniel BM, *et al.* Oxidation increases mucin polymer cross-links to stiffen airway mucus gels. *Sci Transl Med* 2015;7:276ra27.
55. Chen G, Sun L, Kato T, Okuda K, Martino MB, Abzhanova A, *et al.* IL-1β dominates the promucin secretory cytokine profile in cystic fibrosis. *J Clin Invest* 2019;129:4433–4450.
56. Xu Y, Mizuno T, Sridharan A, Du Y, Guo M, Tang J, *et al.* Single-cell RNA sequencing identifies diverse roles of epithelial cells in idiopathic pulmonary fibrosis. *JCI Insight* 2016;1:e90558.
57. Yang J, Zuo WL, Fukui T, Chao I, Gomi K, Lee B, *et al.* Smoking-dependent distal-to-proximal repatterning of the adult human small airway epithelium. *Am J Respir Crit Care Med* 2017;196:340–352.
58. Kurche JS, Dobrinskikh E, Hennessy CE, Huber J, Estrella A, Hancock LA, *et al.* Muc5b enhances murine honeycomb-like cyst formation. *Am J Respir Cell Mol Biol* 2019;61:544–546.
59. Yang C, Zeng HH, Du YJ, Huang J, Zhang QY, Lin K. Correlation of luminal mucus score in large airways with lung function and quality of life in severe acute exacerbation of COPD: a cross-sectional study. *Int J Chron Obstruct Pulmon Dis* 2021;16:1449–1459.
60. Leitz DHW, Duerr J, Mulugeta S, Seyhan Agircan A, Zimmermann S, Kawabe H, *et al.* Congenital deletion of *Nedd4-2* in lung epithelial cells causes progressive alveolitis and pulmonary fibrosis in neonatal mice. *Int J Mol Sci* 2021;22:6146.
61. Zhang Q, Wang Y, Qu D, Yu J, Yang J. The possible pathogenesis of idiopathic pulmonary fibrosis considering *MUC5B*. *BioMed Res Int* 2019;2019:9712464.
62. Naikawadi RP, Disayabutr S, Mallavia B, Donne ML, Green G, La JL, *et al.* Telomere dysfunction in alveolar epithelial cells causes lung remodeling and fibrosis. *JCI Insight* 2016;1:e86704.
63. Wu H, Yu Y, Huang H, Hu Y, Fu S, Wang Z, *et al.* Progressive pulmonary fibrosis is caused by elevated mechanical tension on alveolar stem cells. *Cell* 2020;180:107–121.e17.
64. Miura Y, Lam M, Bourke JE, Kanazawa S. Bimodal fibrosis in a novel mouse model of bleomycin-induced usual interstitial pneumonia. *Life Sci Alliance* 2021;5:e202101059.
65. Hori Y, Imanishi A, Matsukawa J, Tsukimi Y, Nishida H, Arikawa Y, *et al.* 1-[5-(2-Fluorophenyl)-1-(pyridin-3-ylsulfonyl)-1H-pyrrol-3-yl]-N-methyl-methanamine monofumarate (TAK-438), a novel and potent potassium-competitive acid blocker for the treatment of acid-related diseases. *J Pharmacol Exp Ther* 2010;335:231–238.
66. Sakurai Y, Mori Y, Okamoto H, Nishimura A, Komura E, Araki T, *et al.* Acid-inhibitory effects of vonoprazan 20 mg compared with esomeprazole 20 mg or rabeprazole 10 mg in healthy adult male subjects—a randomised open-label cross-over study. *Aliment Pharmacol Ther* 2015;42:719–730.
67. Kawai T, Oda K, Funao N, Nishimura A, Matsumoto Y, Mizokami Y, *et al.* Vonoprazan prevents low-dose aspirin-associated ulcer recurrence: randomised phase 3 study. *Gut* 2018;67:1033–1041.
68. Kojima Y, Takeuchi T, Sanomura M, Higashino K, Kojima K, Fukumoto K, *et al.* Does the novel potassium-competitive acid blocker vonoprazan cause more hypergastrinemia than conventional proton pump inhibitors? A multicenter prospective cross-sectional study. *Digestion* 2018;97:70–75.
69. Miwa H, Uedo N, Watari J, Mori Y, Sakurai Y, Takanami Y, *et al.* Randomised clinical trial: efficacy and safety of vonoprazan vs. lansoprazole in patients with gastric or duodenal ulcers—results from two phase 3, non-inferiority randomised controlled trials. *Aliment Pharmacol Ther* 2017;45:240–252.
70. Ozaki H, Harada S, Takeuchi T, Kawaguchi S, Takahashi Y, Kojima Y, *et al.* Vonoprazan, a novel potassium-competitive acid blocker, should be used for the *Helicobacter pylori* eradication therapy as first choice: a large sample study of vonoprazan in real world compared with our randomized control trial using second-generation proton pump inhibitors for *Helicobacter pylori* eradication therapy. *Digestion* 2018; 97:212–218.
71. Umezawa M, Kawami N, Hoshino S, Hoshikawa Y, Koizumi E, Takenouchi N, *et al.* Efficacy of on-demand therapy using 20-mg vonoprazan for mild reflux esophagitis. *Digestion* 2018;97:309–315.
72. Raghu G, Rochwerg B, Zhang Y, Garcia CA, Azuma A, Behr J, *et al.*; American Thoracic Society; European Respiratory Society; Japanese Respiratory Society; Latin American Thoracic Association. An official ATS/ERS/JRS/ALAT clinical practice guideline: treatment of idiopathic pulmonary fibrosis. An update of the 2011 clinical practice guideline. *Am J Respir Crit Care Med* 2015;192:e3–e19.
73. Ghebremariam YT, Cooke JP, Gerhart W, Griego C, Brower JB, Doyle-Eisele M, *et al.* Pleiotropic effect of the proton pump inhibitor esomeprazole leading to suppression of lung inflammation and fibrosis. *J Transl Med* 2015;13:249.
74. Phathom Pharmaceuticals. Phathom Pharmaceuticals Announces FDA Approval of VOQUEZNA™ triple pak™ (vonoprazan, amoxicillin, clarithromycin) and VOQUEZNA™ DUAL PAK™ (vonoprazan, amoxicillin) for the Treatment of H. pylori Infection in Adults. Florham Park, NJ: Phathom Pharmaceuticals; 2022. [created 2022 May 3; accessed 2022 Nov 21]. Available from: https://investors.phathompharma.com/news-releases/news-release-details/phathom-pharmaceuticals-announces-fda-approval-voqueznatm-triple.
75. Fernandez IE, Eickelberg O. The impact of TGF-β on lung fibrosis: from targeting to biomarkers. *Proc Am Thorac Soc* 2012;9:111–116.
76. Jenkins G. Demystifying pulmonary fibrosis. *Am J Physiol Lung Cell Mol Physiol* 2020;319:L554–L559.
77. Kim KK, Sheppard D, Chapman HA. Tgf-β1 signaling and tissue fibrosis. *Cold Spring Harb Perspect Biol* 2018;10:a022293.
78. Ojiaku CA, Yoo EJ, Panettieri RA Jr. Transforming growth factor β1 function in airway remodeling and hyperresponsiveness. The missing link? *Am J Respir Cell Mol Biol* 2017;56:432–442.
79. Kottmann RM, Kulkarni AA, Smolnycki KA, Lyda E, Dahanayake T, Salibi R, *et al.* Lactic acid is elevated in idiopathic pulmonary fibrosis and induces myofibroblast differentiation via pH-dependent activation of transforming growth factor-β. *Am J Respir Crit Care Med* 2012;186: 740–751.
80. Nocera M, Chu TM. Characterization of latent transforming growth factor-beta from human seminal plasma. *Am J Reprod Immunol* 1995;33: 282–291.
81. Lyons RM, Keski-Oja J, Moses HL. Proteolytic activation of latent transforming growth factor-beta from fibroblast-conditioned medium. *J Cell Biol* 1988;106:1659–1665.
82. Lawrence DA, Pircher R, Jullien P. Conversion of a high molecular weight latent beta-TGF from chicken embryo fibroblasts into a low molecular weight active beta-TGF under acidic conditions. *Biochem Biophys Res Commun* 1985;133:1026–1034.
83. Nayeem SM, Deep S. pH modulates the TGF-β ligands binding to the receptors: a computational analysis. *J Mol Recognit* 2014;27: 471–481.
84. Sutherland LM, Edwards YS, Murray AW. Alveolar type II cell apoptosis. *Comp Biochem Physiol A Mol Integr Physiol* 2001;129:267–285.
85. Li X, Shu R, Filippatos G, Uhal BD. Apoptosis in lung injury and remodeling. *J Appl Physiol (1985)* 2004;97:1535–1542.
86. Wang R, Ibarra-Sunga O, Verlinski L, Pick R, Uhal BD. Abrogation of bleomycin-induced epithelial apoptosis and lung fibrosis by captopril or by a caspase inhibitor. *Am J Physiol Lung Cell Mol Physiol* 2000;279: L143–L151.
87. Kuwano K, Kunitake R, Maeyama T, Hagimoto N, Kawasaki M, Matsuba T, *et al.* Attenuation of bleomycin-induced pneumopathy in mice by a caspase inhibitor. *Am J Physiol Lung Cell Mol Physiol* 2001; 280:L316–L325.
88. Parimon T, Yao C, Stripp BR, Noble PW, Chen P. Alveolar epithelial type ii cells as drivers of lung fibrosis in idiopathic pulmonary fibrosis. *Int J Mol Sci* 2020;21:2269.
89. Sharma V, Kaur R, Bhatnagar A, Kaur J. Low-pH-induced apoptosis: role of endoplasmic reticulum stress-induced calcium permeability and mitochondria-dependent signaling. *Cell Stress Chaperones* 2015;20: 431–440.
90. Park HJ, Lyons JC, Ohtsubo T, Song CW. Acidic environment causes apoptosis by increasing caspase activity. *Br J Cancer* 1999;80: 1892–1897.